

Hera: A Heterogeneity-Aware Multi-Tenant Inference Server for Personalized Recommendations

Yujeong Choi John Kim Minsoo Rhu
School of Electrical Engineering
KAIST
{yjchoi0606, jjk12, mrhu}@kaist.ac.kr

Abstract—While providing low latency is a fundamental requirement in deploying recommendation services, achieving high resource utility is also crucial in cost-effectively maintaining the datacenter. Co-locating multiple workers of a model is an effective way to maximize query-level parallelism and server throughput, but the interference caused by concurrent workers at shared resources can prevent server queries from meeting its SLA. Hera utilizes the heterogeneous memory requirement of multi-tenant recommendation models to intelligently determine a productive set of co-located models and its resource allocation, providing fast response time while achieving high throughput. We show that Hera achieves an average 37.3% improvement in effective machine utilization, enabling 26% reduction in required servers, significantly improving upon the baseline recommendation inference server.

I. INTRODUCTION

Deep neural network (DNN) based personalized recommendation models play a vital role in today’s consumer facing internet services (e.g., e-commerce, news feed, Ads). Facebook, for instance, reports that recommendation models account for more than 75% of all the machine learning (ML) inference cycles in their datacenters [1]. A major challenge facing this emerging ML workload is the need to effectively balance low latency and high throughput. More concretely, unlike training scenarios where throughput is the primary figure-of-merit, ensuring low latency responsiveness is a fundamental requirement for inference services, especially for these user-facing recommendation models. Nonetheless, achieving high server utility and system throughput is still vital for hyperscalers as cost-effectively maintaining the consolidated datacenters directly translates into low total cost of ownership (TCO).

Given this landscape, “co-locating” multiple *workers* from a single or multiple recommendation models is an effective solution to improve system throughput. As the inference server is constantly being fed with numerous service queries, the scheduler can utilize such *query-level parallelism* to have multiple inference queries be *concurrently* processed using these multiple workers. Recommendations are typically deployed using CPUs because of their high availability at datacenters as well as their latency-optimized design. A **key challenge** in co-locating recommendation models over a multi-core CPU is determining which models to co-locate

together, how many workers per each model to deploy, and how to gracefully handle the interference between co-located workers at shared resources, i.e., caches and the memory system. Latency-critical ML tasks operate with strict service level agreement (SLA) goals on tail latency, so even a small amount of disturbance at shared resources can cause deteriorating effects on “latency-bounded” throughput (i.e., the *number of queries processed per second that meets SLA targets*, aka QPS).

To this end, an important motivation and contribution of this work is a detailed characterization on the effect of co-locating multiple recommendation model workers on tail latency as well as latency-bounded throughput. We make several observations unique to multi-tenant recommendation inference. Conventional convolutional and recurrent neural networks (CNNs and RNNs) are primarily based on highly regular DNN algorithms. These “dense” DNN models enjoy high QPS improvements by utilizing query-level parallelism to scale up the number of multi-tenant workers [2], a property this paper henceforth refers to as *worker scalability*. However, DNN-based recommendations employ “sparse” *embedding layers* in addition to dense DNNs, exhibiting a highly irregular memory access pattern over a large embedding table. Depending on which application domain the recommendation model is being deployed (e.g., ranking, filtering, . . .), the configuration of different models can vary significantly in terms of its 1) embedding table size, 2) the number of embedding table lookups per each table, and 3) the depth/width of the dense DNN layers. All these factors determine the memory capacity and bandwidth demands of a model, affecting its worker scalability (Section V). For example, recommendations with a modest model size generally exhibit a compute-limited, cache-sensitive behavior with high worker scalability. On the other hand, models with high memory (capacity and/or bandwidth) requirements are substantially limited with their worker scalability, rendering co-location a suboptimal, or worse, an impossible design point. As a result, blindly choosing the recommendation models to co-locate, without accounting for each model’s worker scalability, leads to aggravated tail latency and QPS, leaving significant performance left on the table.

In this paper, we present *Hera*, a “**H**eterogeneous Memory Requirement Aware Co-location Algorithm” for multi-tenant recommendation inference. The innovation of Hera lies in its ability to accurately estimate *co-location affinity* among

arXiv:2302.11750v1 [cs.DC] 23 Feb 2023

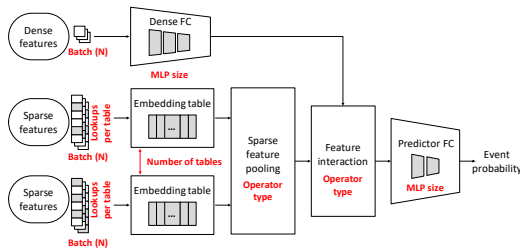


Fig. 1: Model architecture of DNN-based recommendations

a given pair of recommendation models. Models with high (or low) co-location affinity are defined as those that can (or fail to) sustain high QPS while sharing the compute/memory resources with each other. Our **key observation** is that memory capacity and/or bandwidth limited recommendations with low worker scalability generally exhibit high co-location affinity with models with high worker scalability. This is because memory-limited models fail to fully utilize on-chip cores and its local caches, allowing compute-limited/cache-sensitive models to leverage such opportunity to spawn more workers while causing less disturbance to tail latency.

Based on such key observation, we design Hera with two key components: 1) a “cluster-level” model selection unit (Section VI-B) and 2) a “node-level” shared resource management unit (Section VI-C). At the cluster level, Hera utilizes an analytical model that systematically evaluates co-location affinity among any given pair of recommendation models. Hera’s model selection unit then utilizes this information to determine *what models* are most appropriate to be co-located together across all the nodes within the cluster. Once the models to co-locate are determined, Hera’s node-level resource management unit examines *how many workers* as well as *how much shared cache capacity* each model should be allocated within each node that effectively utilize query-level parallelism for high sustained QPS. Overall, Hera achieves an average 37.3% improvement in effective machine utilization, which enables a 26% reduction in the number of required inference servers, significantly improving state-of-the-art.

II. BACKGROUND

A. Neural Recommendation Models

Recommendation models aim to find out contents/items to recommend to a user based on prior interactions as well as user’s preference. A well-known challenge with content recommendations is that users interact only with a subset of available contents and items. Take YouTube as an example where any given user only watches a tiny subset of available video clips. Consequently, state-of-the-art DNN-based recommendation models combine both *dense* and *sparse* features for high accuracy. Here, dense features represent continuous inputs (e.g., user’s age) whereas sparse features represent categorical inputs (e.g., a collection of movies a user has previously watched). Figure 1 shows a high-level overview of DNN-based recommendation models which we detail below.

Model architecture overview. The dense features in recommendations are processed with a stack of dense (bottom)

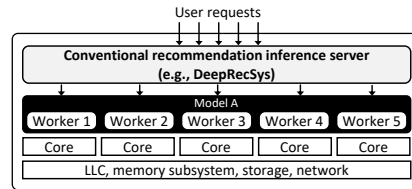


Fig. 2: A CPU-based multi-tenant recommendation inference server.

DNN layers (e.g., convolutions, recurrent, and MLPs). Categorical features on the other hand are encoded as multi-hot vectors where a “1” represent a positive interaction among the available contents/items. As the number of positive interaction among all possible items are extremely small (i.e., a small number of “1”s within the multi-hot vector), the multi-hot vectors are transformed into real-valued, dense vectors (called *embeddings*) by an *embedding layer*. Specifically, an array of embedding vectors are stored contiguously as a table, and a sparse index ID (designating the location of “1”s within the multi-hot vector) is used to read out a unique row from this table. Because the multi-hot vector is extremely sparse, reading out the embedding vectors (corresponding to each sparse indices) from the table is equivalent to a sparse vector *gather* operation. The embedding vectors gathered from a given embedding table are reduced down into a single vector using element-wise additions. In general, embedding vector gather operations exhibit a highly memory-limited behavior as they are highly sparse and irregular memory accesses. Another distinguishing aspect of embedding layers is their high memory capacity demands: the embedding tables can contain several millions of entries, amounting to tens to hundreds of GBs of memory usage.

As there are multiple embedding tables, multiple *reduced* embeddings are generated by the embedding layer, the result of which goes through a feature interaction stage. One popular mechanism for feature interactions is a dot-product operation [3] between all input vectors (i.e., implemented as a batched GEMM). The feature interaction output is concatenated with the output of the bottom DNN layer, which is subsequently processed by the top DNN layers to calculate an event probability (e.g., the click-through-rates in advertisement banners) for recommending contents/items.

State-of-the-art DNN-based recommendation models. While Figure 1 broadly captures the high-level architecture of DNN-based recommendations, state-of-the-art model architectures deployed in industry settings exhibit notable differences in terms of their key design parameters (colored in red in Figure 1). Table I summarizes our studied, industry-scale DNN-based recommendation models published from Google, Facebook, and Alibaba [1], [4], [5], [6], [7]. We further detail our evaluation methodology later in Section IV.

B. Inference Serving Architectures

Why CPUs for recommendation inference? As the complexity of ML algorithms increases, GPUs or dedicated ASICs are gaining momentum in servicing recommendations [8], [9], [10]. Nonetheless, CPUs are still popular deployment

TABLE I: Key architectural configurations of state-of-the-art neural recommendation models.

Model	Domain	FC			Embeddings				SLA (ms)	
		Dense-FC	Predict-FC	Size (MB)	Tables	Lookup	Dimension	Size (GB)		Pooling
DLRM (A)	Social media	128-64-64	256-64-1	0.2	8	80	64	2	Sum	100
DLRM (B)	Social media	256-128-64	128-64-1	0.5	40	120	64	25	Sum	400
DLRM (C)	Social media	2560-1024-256-32	512-256-1	12	10	20	32	2.5	Sum	100
DLRM (D)	Social media	256-256-256	256-64-1	0.2	8	80	256	8	Sum	100
NCF	Movies	-	256-256-128	0.6	4	1	64	0.1	Concat	5
DIEN	E-commerce	-	200-80-2	0.2	43	1	32	3.9	Attention+RNN	35
DIN	E-commerce	-	200-80-2	0.2	4	3	32	2.7	Attention+FC	100
Wide&Deep	Play store	-	1024-512-256	8	27	1	32	3.5	Concat	25

options for several hyperscalars [1], [9], [11], [12], [13], [14] because the abundance of CPUs in today’s datacenters make them appealing from a TCO perspective, particularly during the off-peak portions of the diurnal cycle where they remain idle. In fact, key industrial organizations are constantly developing system-level solutions that better optimize CPU-based recommendation inference [9], [11], [15]. Given their importance in ML inference, this paper focuses on CPU-based inference servers tailored for recommendations.

Multi-tenant inference server architecture. While providing fast response to end-users is vital for inference, achieving high server utility is also crucial for cost-effectively maintaining the consolidated datacenters. Co-locating multiple *workers* of an ML model on a single machine is an effective solution to improve server utility and throughput at the cost of aggravated latency. In our baseline CPU-based, multi-tenant inference server, a single worker (implemented using Caffe2 worker) is allocated with a dedicated CPU core and its local caches, multiples of which share the last level cache (LLC) and the memory subsystem (Figure 2). Because the inference server is consistently being requested with multiple service queries, having multiple workers helps leverage *query-level parallelism* to simultaneously execute multiple inference services, improving throughput. As inference is a highly latency-sensitive operation, existing ML frameworks are designed with an *in-memory* processing model assuming the entire working set of a given worker process is all captured inside DRAM (i.e., paging data in and out of disk swap space is a non-option). Therefore, having multiple workers be co-located within a single machine requires the CPU memory capacity to be large enough to fully accommodate the aggregate memory usage of *all* the concurrent workers [13], [16], [17].

III. RELATED WORK

Improving server cost-efficiency via multi-tenancy has been studied extensively in prior literature [18], [19], [20], [21], [22], [23]. As co-located multi-tenant tasks contend for shared resources, prior work has focused on how to minimize interference and performance unpredictability. A common approach is to co-locate a user-facing, latency-critical task with best-effort workloads (e.g., batch jobs), prioritizing the latency-critical task with higher QoS to meet SLA. While effective in guaranteeing QoS for latency-critical tasks, such solution suffers from low server utility in terms of the number of latency-critical tasks scheduled per servers. Consequently, recent work [24], [25], [26] explored QoS-

TABLE II: CPU server node configuration.

Component	Specification
CPU model	Intel(R) Xeon(R) Gold 6242 CPU
Frequency	2.80 GHz
Physical cores per socket	16
Sockets	2
SIMD	AVX-512
Shared L3 cache size	22 MB (11-ways)
DRAM capacity	192 GB per socket
DRAM speed	2666 MT/s
DRAM bandwidth	128 GB/s
Operating system	CentOS Linux 7
Network bandwidth	10 Gbps

aware resource management techniques that can accommodate *multiple* latency-critical tasks within a single machine. Unlike these prior work focusing on generic, latency-critical cloud services (e.g., Memcached, Sphinx, MongoDB, ...), our work focuses on ML-based recommendation inference servers, presenting our unique, application-aware Hera architecture. More importantly, Hera develops a novel analytical model that quantifies co-location affinity among a given pair of recommendation models for intelligently selecting models to co-locate.

More relevant to Hera is recent work by Gupta et al. [1], [13], which conducts a workload characterization on the effect of co-locating multiple workers from a single, *homogeneous* recommendation model (Figure 2). As we detail in Section V-B, co-locating workers from a single model severely limits the worker scalability for memory capacity or bandwidth limited recommendations. To the best of our knowledge, Hera is the first to quantitatively evaluate the effect of co-locating workers from both homogeneous as well as *heterogeneous* recommendation models, developing a cluster-wide heterogeneous model selection algorithm as well as a node-level QoS-aware resource partitioning algorithm for recommendation inference servers. While not directly related to recommendation inference, Choi et al. [27] and Ghodrati et al. [28] studied an NPU-based multi-tenant inference for CNNs/RNNs/Attentions using temporal [27] and spatial [28] multi-tasking, respectively. There is also several recent work proposing near-data processing for accelerating recommendations [29], [30], [31], [32], [33]. In general, the key contributions of Hera is orthogonal to these prior work.

IV. METHODOLOGY

Hardware platform. We utilize a multi-node cluster containing one master node and five compute nodes, allowing a total of ten inference servers to be deployed (Table II). The intra-node resource partitioning and isolation are done using Linux’s *cpuset cgroups* for allocating specific core IDs to a

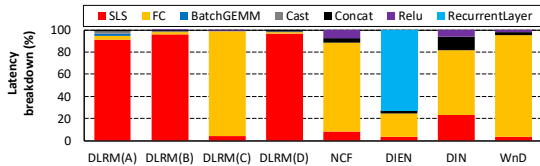


Fig. 3: A single worker’s inference time *without* co-location broken into key operators of Caffe2, assuming a batch size of 220 (mean value of our studied query size distribution, Section IV). Embedding layers are implemented using SparseLengthsSum (SLS) in Caffe2. FC and BatchGEMM refers to fully-connected and batched GEMM.

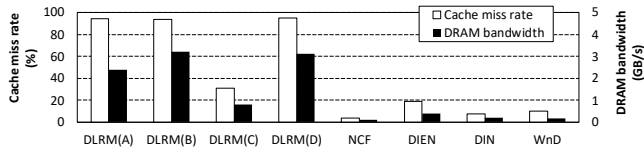


Fig. 4: Effect of single worker inference on on-chip cache miss rate (left) and off-chip DRAM bandwidth utility (right).

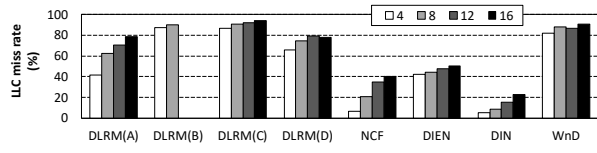
given model worker, and Intel’s *Cache Allocation Technology* (CAT) for LLC partitioning.

Software architecture. Hera’s runtime manager is implemented using Facebook’s open-sourced DeepRecInfra [13], a software framework for designing ML inference servers for at-scale neural recommendation models.

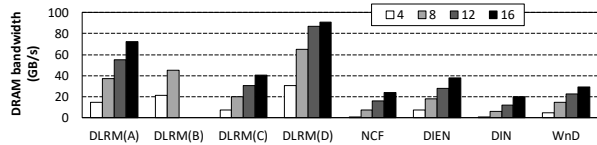
Query arrival rates. Prior work [13] reports that the query arrival rates of recommendation services in a production datacenter follows a Poisson distribution. Similarly, MLPerf’s cloud inference suite [34] also employs a Poisson distribution in its inference query traffic generator. As such, our evaluation utilizes DeepRecInfra’s inference query traffic generator which issues requests to the inference server based on a Poisson distribution, the query arrival rate of which is configured as appropriate per our evaluation goals (detailed in Section VII).

Query working set size. The size of queries for recommendation inference decides the number of items to be ranked for a given user, which determines request batch size. Prior work [13] observes that the working set sizes for recommendation queries follow a unique distribution with a heavy tail effect. We utilize DeepRecInfra to properly reflect such distribution, having the batch size of an inference range from 1-1024 [13].

Benchmarks. We utilize the open-sourced recommendation models provided with DeepRecInfra [13] to construct eight industry-representative model architectures. The SLA target of each model is properly chosen in accordance to prior work [4], [5], [6], [13] (Table I). As discussed in Section II-A, recent literature frequently points to large embedding tables [33], [35], [36], [37] with wide embedding vectors (32 to 1024 dimensions) [29], [38], [39] as it helps improve algorithmic performance. Two of our model architectures accommodate such latest algorithmic developments: 1) DLRM(B) that models similar scale of memory capacity requirement to MLPerf’s DLRM (sized with tens of GBs of embedding tables), and 2) DLRM(D) modeling embeddings with wide vectors.



(a)



(b)

Fig. 5: Effect of scaling up multi-tenant workers on (a) LLC miss rate and (b) memory bandwidth utilization. DLRM(B) does not have bars under 12/16 workers as it results in an out-of-memory error.

V. WORKLOAD CHARACTERIZATION

A. Analysis on “Single” Model Worker

We start by characterizing a single worker’s inference behavior *without* co-location, breaking down latency per major compute operators. As shown in Figure 3, the apparent operator diversity leads to different performance bottlenecks. For example, models such as DLRM(A, B, D) are significantly bottlenecked on the memory intensive embedding layers, experiencing high cache miss rate and high memory bandwidth usage (Figure 4). Because embedding vector gather operations are conducted over a large embedding table, its memory access stream are extremely sparse and irregular with low data locality. Consequently, models with a large number of embedding tables and embedding lookups (DLRM(A, B)) or wide embedding vectors (DLRM(D)) show much higher memory intensity as the majority of execution time is spent gathering embedding vectors. Such property is in stark contrast to DLRM(C), NCF, DIEN, DIN, and WnD, which spend significant amount of time on the computationally intensive FC and/or recurrent layers. Thanks to the (relatively) higher compute intensity and smaller working set, these compute-intensive models exhibit better caching efficiency and lower memory bandwidth consumption.

B. Serving with “Multi”-Tenant Workers

Building on top of the characterization on single worker inference, we now study the efficacy of co-locating *multiple* workers from a *single* recommendation model. We assume a single multi-core CPU machine is utilized for servicing inference queries for the recommendation model but the number of concurrently executing workers are scaled “up” (i.e., one worker per each core, Figure 2) to characterize its effect on shared memory resources (Figure 5) as well as latency-bounded throughput, i.e., QPS (Figure 6). QPS is measured by quantifying the maximum input load the concurrent workers can process without violating SLA. Specifically, we start from a low input query arrival rate (i.e., queries arrived per second) and gradually inject higher request rates until the observed (95th percentile) tail latency starts violating the SLA target.

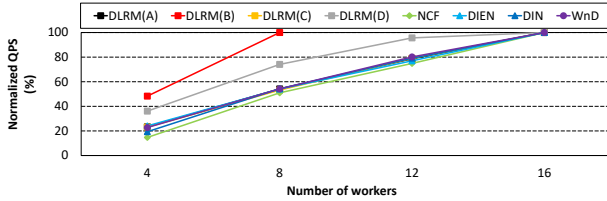


Fig. 6: Latency-bounded throughput (QPS) as a function of the number of parallel workers. We show normalized QPS to 16 workers to demonstrate each model’s worker scalability.

The *max load* of a recommendation model therefore is defined to quantify the maximum input query arrival rate its workers are able to sustain without SLA violation.

As the number of workers are increased, we generally observe a gradual increase in LLC miss rate with a corresponding increase in memory bandwidth usage. This is expected as more workers proportionally demand larger compute and memory usage. However, there are noticeable differences in the way different models react under a multi-tenant inference scenario. First and foremost, memory “capacity” hungry models such as DLRM(B) is severely limited with its ability to spawn a large number of concurrent workers as the aggregate memory usage of a single worker alone amounts to 25 GB (Table I). Consequently, the inference server suffers from an *out-of-memory* error beyond 8 workers (recall that ML inference servers employ a software stack implemented using an in-memory processing model, Section II-B), leaving an average 50% of CPU cores and on-chip caches left idle. Such behavior is likely to be a significant concern to hyperscalers because recent literature frequently points to neural recommendation models having several tens to hundreds of GBs of memory usage [1], [36], [37], [40]. As such, co-locating a large number of workers for these memory capacity limited models are challenging under current ML serving architectures (Figure 6). Second, embedding limited models with high memory “bandwidth” usage (DLRM(A, D)) exhibit an almost linear increase in memory bandwidth utility with a large number of workers. This is because the LLC fails to capture the already meager data locality of embedding layers, frequently missing at the LLC and consuming high memory bandwidth. The performance of DLRM(D) in particular is completely bottlenecked on memory bandwidth, whose aggregated bandwidth usage saturates beyond 12 workers (Figure 5). As a result, the QPS improvements in DLRM(D) levels off around 12 workers, only achieving a further 4% throughput enhancements going from 12 to 16 workers. Therefore, scaling up the number of multi-tenant workers beyond 12 for DLRM(D) is highly sub-optimal from a throughput cost-efficiency perspective. Lastly, the remaining five recommendation models with high compute intensity and a modest model size (Table I) leave plenty of memory bandwidth available even when the number of parallel workers are maximized. As shown in Figure 6, such headroom in memory bandwidth allows these compute-intensive recommendation models to enjoy a scalable increase in QPS with a large number of parallel workers.

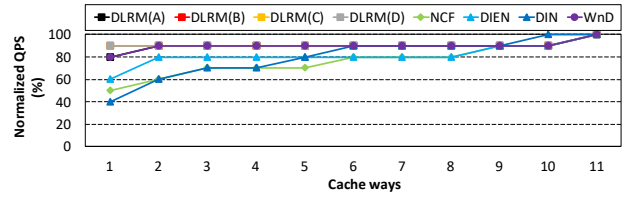


Fig. 7: Changes in latency-bounded throughput (QPS) when limiting the number of LLC ways allocated to workers. Results are normalized to the right-most configuration where we allow the workers to fully utilize the entire (11 ways) LLC. Each experiment assumes maximally possible workers are spawned for execution (8 for DLRM(B) and 16 for other models). Note that Intel’s CAT prevents the allocation of *zero* LLC ways to any given process (i.e., *bypassing* the LLC is impossible), thus having at least a single LLC way allocated per each model is required. We observed similar trends when measuring sensitivity of QPS on LLC over different number of workers, so we omit them for brevity.

Overall, we conclude that recommendation models with high memory capacity and/or bandwidth demands are severely limited with its *worker scalability*, i.e., the ability to leverage query-level parallelism in ML inference servers to scalably increase QPS via multi-tenant workers. In contrast, models that are relatively more compute intensive with high cache sensitivity exhibit much better worker scalability. Such high worker scalability however is only guaranteed when each worker is provided with a “large enough” LLC capacity to sufficiently capture locality, as we further discuss below.

C. Sensitivity to LLC Capacity

To analyze the sensitivity of each model’s worker scalability to LLC size, we utilize Intel’s Cache Allocation Technology (CAT) [41] to limit the number of LLC ways allocated to the multi-tenant workers. Figure 7 plots the sustained QPS of each model architecture (y-axis) as we gradually limit the number of ways allocated to the executing workers (from right to left on the x-axis). Several important observations can be made from this experiment. First, the memory-limited DLRM(A, B, D) shows high robustness to available LLC capacity. For instance, DLRM(D) is able to achieve 90% of maximum QPS despite having only a single LLC way allocated. These memory-limited models spend significant fraction of their execution time on highly irregular embedding gather operations with low locality (Figure 3). Therefore, leveraging memory parallelism rather than locality (i.e., memory bandwidth rather than LLC capacity) is more crucial for these memory-limited models in achieving high sustained QPS. Second, models with high compute-intensity (NCF, DIEN, DIN, WnD) exhibit high sensitivity to the LLC capacity, underscoring the importance of sufficiently provisioning shared cache space to the multi-tenant workers. Interestingly, many of these cache-sensitive workloads are able to sustain reasonably high QPS despite having allocated with a small LLC space. For instance, DIEN is capable of achieving more than 80% of maximum QPS while only being allocated with 2 out of the 11 LLC ways (and similarly 2 ways and 5 ways for WnD and DIN, respectively).

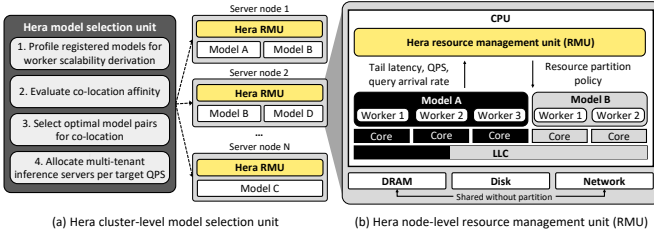


Fig. 8: High-level overview of Hera architecture.

VI. HERA ARCHITECTURE AND DESIGN

A. Design Principles

Overview. Figure 8 provides an overview of Hera’s two key components, 1) the *cluster-level* model selection unit (Section VI-B) and 2) the *node-level* shared resource management unit (Section VI-C). At the cluster level, Hera employs our analytical model that utilizes the heterogeneous memory needs of recommendations for selecting the optimal pair of models to co-locate across all the server nodes. Once the models to co-locate are determined, Hera node-level resource management unit sets up the proper compute/memory resource allocation strategy for the multi-tenant workers, which is dynamically tuned for maximum efficiency by closely monitoring each model’s tail latency, QPS, and query arrival rates.

Key approach. Section V-B revealed that models with high memory capacity or bandwidth usage suffer from low worker scalability, leaving significant amount of CPU cores and shared LLC underutilized. To address such inefficiency, Hera aims to deploy workers from a pair of low and high worker scalability models, as their complementary compute and memory usage characteristic (i.e., memory-intensive vs. compute-intensive execution for low vs. high worker scalability models respectively) helps maximize server utility while minimizing interference at shared resources. Figure 9 provides examples that highlight the importance of Hera’s worker scalability aware, multi-tenant model selection algorithm, where the cache-sensitive NCF is co-located with (a) another cache-sensitive DIEN and (b) memory capacity limited DLRM(B). As depicted, co-locating two cache-sensitive and high worker scalability models with similar resource requirements (NCF and DIEN) results in severe interference at the LLC, causing an average 20% throughput loss compared to each model’s isolated execution. In contrast, consider the example in Figure 9(b) where workers with complementary compute/memory access patterns are co-located. Because of DLRM(B)’s memory capacity constraints, the model is not able to fully utilize the 16 cores on-chip, rendering the remaining CPU cores and LLC left underutilized. Co-locating NCF with DLRM(B) therefore helps better utilize server resources thereby significantly improving aggregate throughput. Of course, the interference between DLRM(B) and NCF cannot be eliminated completely, so both models experience some throughput loss compared to their respective isolated executions. Nonetheless, the net benefit of enhanced

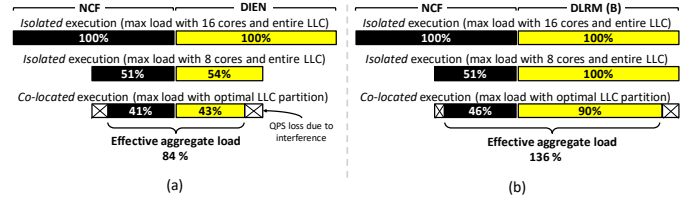


Fig. 9: Effect of co-locating (a) (high, high) worker scalability models and (b) (high, low) worker scalability models.

server utility via intelligently co-locating low and high worker scalability models outweighs the deterioration in each model’s throughput, leading to a significant system-wide QPS improvement.

As such, we seek to address the key research challenge regarding how to reliably estimate a given model’s worker scalability and utilize that information to decide the optimal set of models to co-locate across the cluster. Once the models to co-locate are determined, another research question remains regarding how to efficiently allocate shared resources among multi-tenant workers that minimize interference and maximize QPS. We first elaborate on Hera’s cluster-level model selection algorithm in Section VI-B followed by a discussion of our node-level resource management policy in Section VI-C.

B. Cluster-level Multi-tenant Model Selection Unit

Profiling-based worker scalability estimation. Through our characterization in Section V-B, we observe that a given recommendation model’s performance scalability (as a function of the number of concurrent workers) can be estimated reliably through profiling. Hera utilizes the slope of the performance scalability curve in Figure 6 to make a binary decision on whether the subject model has high worker scalability or not. For example, memory capacity limited DLRM(B) and memory bandwidth limited DLRM(D) are categorized as those with low worker scalability because employing a large number of workers is either impossible (DLRM(B)) or simply unproductive beyond a certain threshold from a QPS perspective (DLRM(D)). The remaining recommendation models on the other hand are categorized as having high worker scalability as they can fully utilize the CPU cores and on-chip caches with sustained high QPS. The profiled result in Figure 6 only needs to be collected once for a target server architecture and the derivation of whether a model has high worker scalability or not is entirely done offline, having negligible impact on Hera’s performance or memory usage, i.e., a static boolean variable per each model designates its worker scalability.

Determining key sources of resource contention. By utilizing the recommendation model’s (high/low) worker scalability information, Hera tries to co-locate a pair of (high, low) worker scalability models. This helps us significantly reduce the model selection search space as it tries to avoid the unfruitful co-location of (high, high) worker scalability models. Nonetheless, different recommendation models naturally exhibit different compute and shared resource usage,

Algorithm 1 Co-location Affinity

```

1: ▷ Step A: Derive co-location affinity at LLC
2:  $CoAff_{LLC} = 0$ 
3: for  $i = 1$  to  $CacheWay_{max}$  do
4:    $CacheWay_A = i$ 
5:    $CacheWay_B = CacheWay_{max} - CacheWay_A$ 
6:    $CoAff_{temp} =$ 
    $(\frac{QPS[Model_A][CacheWay_A]}{QPS[Model_A][CacheWay_{max}]} + \frac{QPS[Model_B][CacheWay_B]}{QPS[Model_B][CacheWay_{max}]})/2$ 
7:   if  $CoAff_{temp} > CoAff_{LLC}$  then
8:      $CoAff_{LLC} = CoAff_{temp}$ 
9:   end if
10: end for
11:
12: ▷ Step B: Derive co-location affinity at memory bandwidth
13:  $CoAff_{DRAM} = \min(\frac{MemBW_{system}}{MemBW_A + MemBW_B}, 1)$ 
14:
15: ▷ Step C: Estimation of system-level co-location affinity
16:  $CoAff_{system} = \min(CoAff_{LLC}, CoAff_{DRAM})$ 

```

so understanding a model’s unique resource requirement helps better estimate the magnitude of shared resource contention, thereby narrowing down the model selection search space even further. Prior work [20], [24], [25] considers the shared LLC, memory, storage, and network bandwidth as one of the most important sources of resource contention under multi-tenancy. However, our key finding is that the multi-tenant workers for recommendation inference rarely compete for storage and network bandwidth. As previously discussed in Section II-B, state-of-the-art ML frameworks for inference servers employ an in-memory processing model. Consequently, once the ML inference server is bootstrapped for deployment (e.g., initializing inference server-client processes, provisioning each worker’s memory allocation needs inside DRAM, . . .), the multi-tenant workers have little to no interaction with the storage system at inference time. This is not surprising given the latency-critical nature of inference and its need for high performance predictability. When it comes to the network stack, the ML inference server receives client’s service queries through the NIC over an HTTP/REST protocol [16], [17]. However, we observe less than an average 1.9 Gbps of network bandwidth usage in all our evaluation, far less than the available system-wide network bandwidth (which is typically in the orders of several tens to hundreds of Gbps in at-scale datacenters). Consequently, Hera only considers the interference at shared LLC and memory bandwidth for evaluating both the candidate models for co-location and the efficient resource allocation mechanism for those models. Compared to previous, *generic* QoS-aware resource partitioning mechanisms [20], [24] that consider the interference at all of cache/memory/storage/network, Hera’s *application-awareness* helps our proposal more agilely adapt to the dynamics of inference query arrival patterns, significantly improving upon state-of-the-art (Section VII-A2).

Identifying co-location affinity for model selection. We develop an analytical model that estimates *co-location affinity* among a given pair of models. Hera’s model selection unit utilizes co-location affinity to determine the best set of models to co-locate, choosing those with high co-location affinity, i.e., ones that can sustain high QPS while sharing the

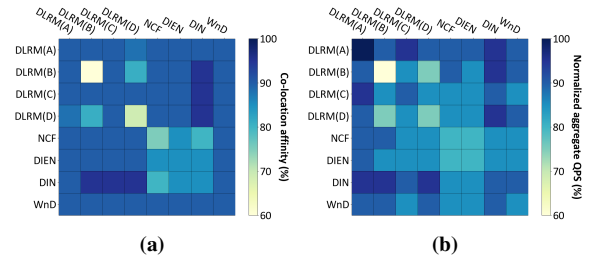


Fig. 10: In (a), we show the *estimated* co-location affinity among all possible pairs of co-located models (the higher the better). To demonstrate how well our co-location affinity models the effect of shared resource interference, we show in (b) the *measured* aggregate QPS of co-located models normalized to the summation of the QPS achieved when each model is executed in isolation.

LLC/memory. Co-location affinity is derived by estimating how much QPS loss is expected to the co-located $Model_A$ and $Model_B$ due to the interference at the shared LLC and memory bandwidth – the two most important sources of resource contention under multi-tenant ML inference (Algorithm 1). Similar to our definition of worker scalability, we employ a profiling-based approach to model the effect of shared resource contention on QPS. First, the profiled LLC sensitivity study in Figure 7 is utilized to derive the expected QPS when $Model_A$ and $Model_B$ gets an equal partition of the CPU cores for worker allocation. Each model is then given a partitioned slice of the shared LLC ways ($CacheWay_A$ and $CacheWay_B$ in line 4-5). The profiled QPS for each model is then normalized to the QPS achieved when each model is given the entire LLC for execution, the result of which is averaged over the two co-located models to quantify the effect of LLC interference (line 6). By examining all possible combination of LLC partitioning, we are able to derive the most optimal LLC partitioning point that gives the highest aggregate QPS (line 7-8). As Hera’s resource management unit is capable of utilizing such information for optimal LLC partitioning (detailed in Section VI-C), we utilize this LLC partitioning point as the reference to quantify co-location affinity at LLC. As such, the closer the $CoAff_{LLC}$ value is to 1, the more likely the co-located models are less interfering with each other, thus having high co-location affinity at LLC.

Estimating co-location affinity for memory bandwidth sharing ($CoAff_{DRAM}$) by following the same measure as done in deriving $CoAff_{LLC}$ is challenging. This is because there is currently no practical way to manually partition and isolate each model’s memory bandwidth usage (unlike the LLC where Intel’s Cache Allocation Technology [41] provides means to fine-tune LLC partitioning). We therefore employ the analytical model in line 13 which utilizes our profiled result in Figure 5(b) to measure co-location affinity with respect to memory bandwidth sharing. Here $MemBW_A$ and $MemBW_B$ are the amount of memory bandwidth consumed when each model is given half of the CPU cores and the entire LLC for isolated execution without co-location. By normalizing the sum of $MemBW_A$ and $MemBW_B$ to the available socket-level memory bandwidth ($MemBW_{system}$), we get an estimate on how much *effective* bandwidth each model will be able to utilize vs. an idealistic scenario without

Algorithm 2 Hera Cluster Scheduling Algorithm

```
1: TargetQPS[m1, m2, ..., mn] = [QPSm1, QPSm2, ..., QPSmn]
2: ServicedQPS[m1, m2, ..., mn] = [0, 0, ..., 0]
3: Low = [models with low worker scalability]
4: High = [models with high worker scalability]
5:
6: ▷ Step A: Allocate servers to be co-located with low worker scalability models
7: for mi in Low do
8:   while ServicedQPS[mi] < TargetQPS[mi] do
9:     mj = find_model_with_highest_colocation_affinity(mi, High)
10:    AllocateNewServer(mi, mj):
11:    // qpsmi, qpsmj : maximum QPS when mi & mj are co-located
12:    ServicedQPS[mj] += qpsmi
13:    ServicedQPS[mi] += qpsmj
14:  end while
15: end for
16:
17: ▷ Step B: Allocate servers for high worker scalability models
18: for m in High do
19:   while ServicedQPS[m] < TargetQPS[m] do
20:     AllocateNewServer(m)
21:     // qpsm : maximum QPS when m is executed in isolation
22:     ServicedQPS[m] += qpsm
23:   end while
24: end for
```

bandwidth interference due to co-location (line 13). The evaluated $CoAff_{DRAM}$ can therefore provide guidance on how intrusive the memory bandwidth sharing will have on co-located models, quantifying co-location affinity at memory. For a conservative evaluation of co-location affinity that considers interference at both LLC and memory, we choose the lower value among the $CoAff_{LLC}$ $CoAff_{DRAM}$ (line 16). Figure 10(a) plots the derived co-location affinity for all possible model pairs we study. To visualize how well our co-location affinity captures the interference and its effect on QPS, we also show in Figure 10(b) the *measured* aggregate QPS of co-located models normalized to the theoretically maximum QPS achievable when each model is executed in isolation. As shown, Figure 10 clearly demonstrates the strong correlation between our estimated co-location affinity and the measured QPS (i.e., Pearson correlation coefficient: 0.95)

It is worth pointing out that the parameters to derive Algorithm 1 are all statically determined. Therefore, the derivation of co-location affinity for all possible model pairs are done offline and are stored as a lookup table inside a two-dimensional array (indexed using $Model_A$ and $Model_B$'s identifier, Figure 10(a)). This table is then utilized by the central master node with global cluster visibility to determine model pairs to co-locate in inference servers to achieve a cluster-wide target QPS. Algorithm 2 is a pseudo-code of Hera's cluster scheduling algorithm where we start by examining the low worker scalability models for deployment, checking the co-location affinity table to find the best candidate for co-location (line 6). Specifically, the scheduler prioritizes models with high worker scalability as prime candidates for co-location with low worker scalability models. When low worker scalability models are all deployed, the remaining models are allocated with a dedicated server in isolation but with maximum workers spawned to maximize QPS (line 17).

Algorithm 3 Hera Resource Management Algorithm

```
1: procedure RESOURCE_MANAGEMENT_ROUTINE()
2:   while True do
3:     ▷ Step A: Monitor phase
4:     Monitor tail latency, QPS, and query traffic rate for Tmonitor
5:     ▷ Step B: Adjust phase
6:     for each model M do
7:       slack = tail_latencyM/SLAM
8:       if slack > 1.0 or slack < 0.8 then
9:         adjust_workers(M)
10:      end if
11:    end for
12:    if number of workers have changed then
13:      adjust_LLC_partition()
14:    end if
15:  end while
16: end procedure
17:
18: procedure ADJUST_WORKERS(m)
19:   urgency = tail_latencym/SLAm
20:   if urgency < 1.0 then
21:     urgency = 1
22:   end if
23:   adjusted_traffic = urgency × trafficquery
24:   number_of_workers = find_number_of_workers(m, adjusted_traffic)
25:   Allocate Model m with number_of_workers
26: end procedure
27:
28: procedure ADJUST_LLC_PARTITION()
29:   QPShighest = 0
30:   for i = 1 to CacheWaymax do
31:     CacheWayA = i
32:     CacheWayB = CacheWaymax - CacheWayA
33:     QPScurr =
34:     QPS[ModelA][Number of workers allocated for ModelA][CacheWayA] +
35:     QPS[ModelB][Number of workers allocated for ModelB][CacheWayB]
36:     if QPScurr > QPShighest then
37:       QPShighest = QPScurr
38:       best_partition = (CacheWayA, CacheWayB)
39:     end if
40:   end for
41:   Allocate ModelA and ModelB with best_partition
42: end procedure
```

C. Node-level Resource Management Unit

Once the model pair to co-locate are chosen for an inference server, Hera goes through the server *initialization* procedure for bootstrapping, followed by an iterative *monitor-and-adjust* process to periodically fine-tune the resource allocation policy per inference query traffic (Figure 8).

Initialization. Server bootstrapping is done by evenly partitioning the CPU cores and shared LLC among the co-located workers (i.e., one core per each worker, all workers for a single model allocated with half the LLC), properly allocating the required data structures *in-memory*. If one of the co-located model does not have enough worker scalability to fully utilize allocated cores (e.g., memory capacity limited DLRM(B)), the *other* model utilizes those idle cores to spawn more workers.

Monitor. After server initialization, Hera resource management unit (RMU) periodically monitors tail latency, QPS, and the service query traffic rate for a period of $T_{monitor}$ to evaluate the effectiveness of current resource allocations (line 4 in Algorithm 3). The RMU checks whether the current core/LLC allocation is appropriate or not by calculating the SLA slack, i.e., ratio between measured latency vs. the model's SLA target (line 7). If the tail latency is larger than the SLA, the RMU deems that the current resource allocation

is under-provisioned and the likelihood of violating SLA is too high. Contrarily, if the tail latency is smaller than the SLA, the possibility of SLA violation is relatively low. However, too large of an SLA slack by some predefined threshold (80% of SLA in our default setting) also implies that the current resource allocation is unnecessarily over-provisioned. Therefore, when either one of these conditions are met for a given model (line 8), RMU calls functions `adjust_workers()` and `adjust_LLC_partition()` to properly upsize/downsize the allocated cores and LLC to make sure they are given sufficient amount of resources to meet SLA (line 9,13).

Adjusting model workers. At-scale datacenters receive a dynamically fluctuating query arrival patterns following a Poisson distribution (Section IV). SLA violations occur because the rate at which inference queries arrive to the server is overwhelmingly too high for the currently available workers. Therefore, the ability to dynamically provision a proportional amount of workers and LLC per query arrival rate is crucial for appropriately handling query-level parallelism. Now recall that our characterization on worker scalability (the left-axis in Figure 6) provides a proxy on how much sustained QPS can be achieved with a given number of workers. The RMU therefore utilizes the performance scalability curve in Figure 6 (the same data structure used in Section VI-B for deriving models’ worker scalability) to find out the minimum number of workers that can achieve sustainable QPS for the current input query arrival rate, `traffic_query` (`find_number_of_workers()` in line 24), the result of which is used to adjust the number of workers for the next monitoring phase. Given the reactive nature of Algorithm 3 (i.e., allocating additional workers occur *after* SLA violation is observed), we additionally define *urgency* of a model’s queries as defined in line 19-21 to make sure Hera can adequately handle high spikes in query arrival rates. We define urgency as the ratio between the measured tail latency and the SLA target, so the higher the urgency the more likely that the inference server has delinquent service queries yet to be serviced inside the server request queue, leading to an unusually high tail latency. By artificially scaling up the observed query traffic rate with its urgency, the RMU helps better provision large enough workers for urgent models, enabling agile responsiveness. Of course, such over-provisioning might lead to unnecessarily large SLA slack after adjustment, but such case is gracefully handled by the RMU by properly downsizing the workers during the next monitor-and-adjust phase.

Adjusting LLC partitions. When the number of workers for each co-located model has changed, the RMU also adjusts the partitioned LLC ways as appropriate using `adjust_LLC_partition()`. Similar to how the optimal LLC way partitioning design point in Algorithm 1 was derived, we employ a profiling-based strategy. Specifically, a one-time, offline profiling of QPS for all the models for all possible combination of (number of workers, number of LLC ways) is conducted, which is used to populate

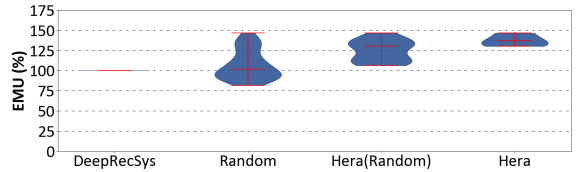


Fig. 11: Violin plots of EMU with constant load. The three markers represent min, median, and max EMU.

the (three-dimensional) lookup table utilized in line 33 of Algorithm 3. Whenever `adjust_LLC_partition()` is called, the RMU utilizes this lookup table to re-evaluate the optimal number of LLC ways to allocate under the renewed (upsized/downsized) number of workers allocated for each model that results in the highest aggregate QPS. The overhead of generating this lookup table is amortized over all future deployments over a target server architecture and the memory allocation required to store this data structure is less than 2 KBs, having negligible impact on performance and memory usage.

VII. EVALUATION

Our evaluation takes a bottom-up approach, first focusing on intra-node evaluation (Section VII-A, Section VII-B), followed by our cluster-wide analysis (Section VII-C). Following prior work [24], we first evaluate scenarios where the multi-tenant workers run at constant loads (Section VII-A) and later explore fluctuating load (Section VII-B).

A. Constant Load

1) *Effectiveness of Hera Model Selection Unit:* We establish two baseline model selection algorithms and two Hera based design points as follows. The baseline designs are: 1) state-of-the-art DeepRecSys [13], which co-locates multiple workers from a single, *homogeneous* model (Section III/Section V-B), and 2) *randomly* choosing any given pair of *heterogeneous* models to co-locate without any restriction (Random). The two Hera design points are 3) Hera (Random) and 4) Hera, where both utilize the worker scalability of the candidate model to avoid the undesirable co-location of (high, high) worker scalability models. However, Hera (Random) randomly chooses any one of the possible model pairs (excluding (high, high) model pairs), whereas Hera can utilize our estimated co-location affinity (Figure 10) to choose model pairs that provide the *highest* machine utilization. To rule out the effect of resource management policy in our evaluation, all four design points including Hera employ our proposed resource management algorithm in Section VI-C.

We measure *Effective Machine Utilization* (EMU), a metric used in related prior work [20], [24], [25] that is defined as the max aggregate load of all co-located applications, where each application’s load is expressed as a percentage of its *max load* when executed in isolation with all server resources (Figure 9, Section V-B discusses how max load is measured for each model). Note that EMU can be above 100% by better bin-packing shared resources among co-located models.

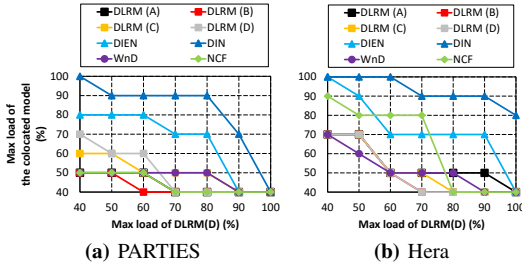


Fig. 12: Each plot shows the result of co-locating the memory bandwidth limited DLRM(D) ($Model_x$) with each of our studied recommendation models ($Model_y$) using (a) PARTIES and (b) Hera. Each line shows the maximum percentage of $Model_y$'s *max load* (y-axis) that can be achieved without SLA violation when $Model_x$ (i.e., DLRM(D)) is running at the fraction of its own *max load* indicated on the x-axis. Therefore, the aggregation of max load for $Model_x$ and $Model_y$ at a particular design point equals its EMU. For instance, the EMU of DLRM(D) and NCF when DLRM(D) is at 50% max load is $(50+50)=100\%$ under PARTIES, while Hera achieves $(50+80)=130\%$.

Figure 11 shows the distribution of EMU for each model selection algorithm's all chosen pair of co-located models. Because DeepRecSys does not co-locate workers from multiple models, QPS is always identical to the max load of isolated execution, thus having EMU of 100%. As for Random, we show the EMU distribution for all possible combination of model pairs among the eight models we study, achieving 82 to 147% EMU. Although Random can improve EMU when opportunistically co-locating low worker scalability models with other models, it fails to rule out the co-location of (high, high) scalability co-location pairs with low co-location affinity, resulting in worst-case 18% EMU loss.

The two Hera design points on the other hand utilizes worker scalability to successfully rule out model pairs with low co-location affinity, guaranteeing the EMU never falls below 100% and achieve substantial EMU improvement than DeepRecSys and Random. However, a key difference between Hera(Random) and Hera are the following. When the cluster-level scheduler selects model pairs to co-locate, Hera(Random) makes random selection from any model combinations except (high, high) worker scalability model pairs. In contrast, Hera utilizes the estimated co-location affinity to judiciously choose model pairs with the highest EMU, leading to significant EMU improvements vs. the other three data points. Overall, Hera achieves 37.3%, 34.7%, and 5.4% average EMU improvement than DeepRecSys, Random, and Hera(Random), respectively.

2) *Effectiveness of Hera Resource Manager:* PARTIES [24] is a QoS-aware intra-node resource manager targeting generic, latency-critical cloud services. To clearly demonstrate the novelty of Hera's application-aware resource manager, we implement PARTIES on top of Hera's model selection algorithm and compare its EMU against Hera. Across all evaluated scenarios, Hera achieves an average 12% (maximum 55%) EMU improvement than PARTIES. Due to space constraints, we show in Figure 12 a subset of our evaluation

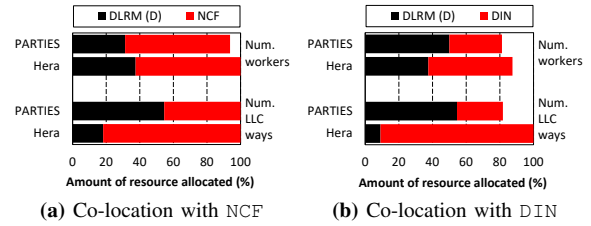


Fig. 13: Number of workers and LLC ways allocated when the low worker scalability DLRM(D) with 50% max load is co-located with high worker scalability (a) NCF and (b) DIN. Hera successfully allocates sufficient number of workers and LLC ways, reaching 80%/100% of max load for NCF/DIN. PARTIES fails to provision high enough LLC to cache-sensitive NCF/DIN, only achieving 50%/90% of max load for these two models.

where we visualize the max load of low worker scalability DLRM(D) (x-axis) and the other co-located model (y-axis). Hera generally achieves higher sustained max load over PARTIES for the majority of design points when gradually injecting each model with loads from 40% to 100% of their respective max load. The reason behind Hera's superior performance is twofold. First, Hera is based on our profile-based characterization to determine a good initial starting point within the search space to find the optimal core/LLC resource allocation scheme. Second, while PARTIES needs to carefully fine-tune all shared resources in a system (i.e., in addition to core/LLC, the disk and network bandwidth is also carefully monitored and adjusted by PARTIES), our application-aware Hera leverages the unique properties of ML inference servers (e.g., in-memory processing, Section VI-B) to narrow down the resource management targets, thus enabling rapid determination of an optimal resource management strategy that best suits recommendation model's heterogeneous memory needs. In Figure 13, we show a snapshot of PARTIES vs. Hera's resource allocation when the low worker scalability DLRM(D) is co-located with high worker scalability NCF and DIN. Given its cache sensitive property (Figure 7), NCF and DIN require sufficient LLC capacity to sustain high max load. While PARTIES is able to eventually allocate enough workers for NCF, the amount of LLC provisioned for this cache-sensitive workload is much lower than under Hera, failing to achieve high max load.

B. Fluctuating Load

This section evaluates the robustness of Hera's resource manager vs. PARTIES in handling dynamically changing query arrival rates. At-scale datacenter applications frequently experience fluctuations in their load (e.g., sudden burst of high traffic load, diurnal patterns where load is high at daytime while gradually decreasing during night time). To simulate such scenario, we employ measures proposed by Chen et al. [24] where we co-locate models with heterogeneous resource requirements, e.g., DLRM(D) and NCF, and vary the query arrival rate as illustrated in Figure 14: the load to both DLRM(D) and NCF are gradually increased until T_1 , which is when NCF experiences a sudden decrease in its load. At T_2 , the query arrival rate to NCF is suddenly spiked from

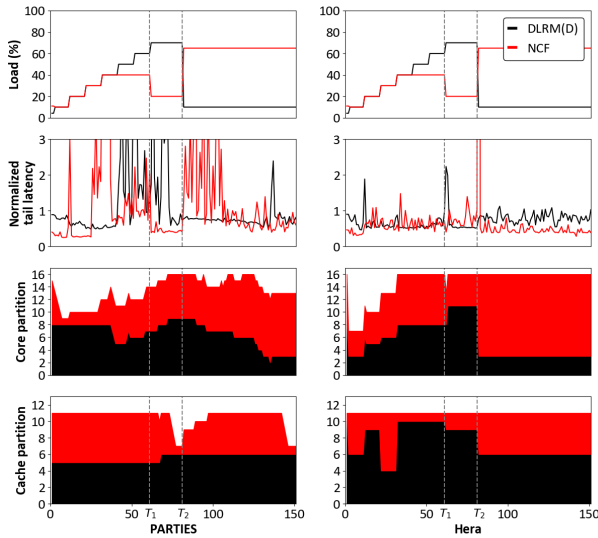


Fig. 14: Changes in tail latency and resource allocations with Hera and PARTIES with fluctuating load for DLRM(D) and NCF. Tail latency is normalized to each model’s respective SLA targets, i.e., normalized latency larger than 1.0 signifies a QoS violation. Note that the maximum number of cores and LLC ways is 16 and 11 under our studied evaluation (Table II).

20%→60% of its max load while DLRM(D) sees a sudden drop from 70%→10%. Figure 14 clearly shows that Hera does a much better job in maintaining tail latency at below SLA, unlike PARTIES which frequently exhibits sudden spikes of SLA violations throughout its execution. Our analysis revealed that PARTIES, while it *is* capable of eventually figuring out a decent resource allocation strategy, the decision is based on a constant upsize/downsize feedback loop that monitors various shared resources within the system. Because Hera utilizes the profile-based characterization lookup table (Algorithm 3), it is able to rapidly determine the optimal resource allocation even at sudden changes of loads at T_1 and T_2 , enabling robust execution even under fluctuating query arrival rates.

C. Cluster-wide Server Utilization

In this section, we analyze Hera’s effectiveness in reducing the number of servers required to fulfill a *cluster-wide* target QPS goal. Because the set of models deployed by hyper-scalers as well as each model’s expected service demand (i.e., query arrival rate) are proprietary information not publicly available, we take the following measure for our evaluation.

Even distribution of target QPS among models. We first assume that the eight models in Table I have an *identical* level of target QPS (Figure 15). We then utilize the four model selection algorithms to measure the total number of servers required to satisfy this target QPS. When the aggregate target QPS across all the models exceeds the max load serviceable by our multi-node cluster, we run separate rounds of experiments in an iterative manner to quantify how many additional servers are needed to service the remaining QPS.

The baseline DeepRecSys allocates a single server to service a single model, so low worker scalability models like DLRM(B, D) require a larger number of servers to reach the

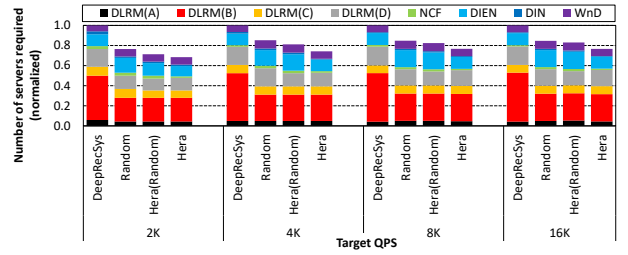


Fig. 15: The number of servers required (y-axis) to service a target QPS level (x-axis) when the target QPS per each model is evenly distributed in an identical manner.

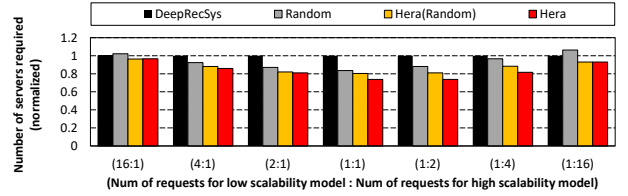


Fig. 16: The number of servers required (y-axis) when low and high worker scalability models have different ratios of target QPS levels (x-axis).

target QPS. As for Random, the cluster scheduler randomly selects a given pair of models for multi-tenant deployment until the target QPS is achieved. Because Random is capable of better utilizing compute nodes servicing low worker scalability models like DLRM(B, D), it is able to reduce the number of servers by an average 15% compared to DeepRecSys. However, Random is not able to properly isolate the interference at shared resources, so the unproductive co-location of (high, high) worker scalability models suffers from low efficiency. Both Hera(Random) and Hera are worker scalability aware and can potentially avoid deploying model pairs with low co-location affinity (e.g., NCF vs. DIEN/DIN/WnD). Nonetheless, Hera does a much better job reducing the number of servers vs. Hera(Random) as it effectively utilizes our estimated co-location affinity to minimize unfruitful model co-location pairs. For instance, Hera noticeably reduces the number of servers utilized for deploying DIEN all thanks to its ability to better bin-pack the shared resources among co-located models, achieving an average 26% and 11% reduction in total required servers than DeepRecSys and Random, respectively.

Skewed distribution of target QPS among models. Figure 16 shows the number of servers needed when the per-model target QPS exhibits a skewed distribution. Unless the queries are *all* requested to low worker scalability models or all to high scalability models (which is unlikely the common case in real-world settings), Hera is able to noticeably reduce the number of servers required to reach a target QPS.

D. Sensitivity

Effect of Hera co-location and LLC partitioning. Hera consists of two key components: 1) affinity-aware co-location algorithm, and 2) application-aware LLC partitioning via Intel CAT. To clearly quantify where Hera’s main benefits come from, we quantify the impact of isolating our two main

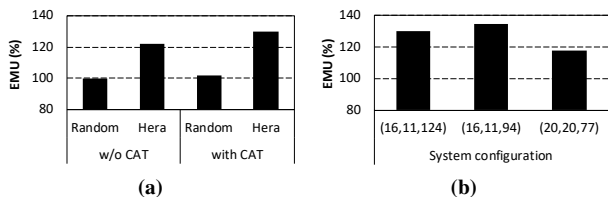


Fig. 17: Hera sensitivity to (a) enabling/disabling LLC partitioning (with and w/o CAT), and (b) different system configurations (the numbers inside the bracket refers to (number of cores, number of LLC ways, and memory bandwidth (GB/sec))). Note that the scale of the y-axis is 80–140%.

proposals in Figure 17(a) as an ablation study. Even without LLC partitioning, Hera’s co-location algorithm alone provides 22% EMU improvements vs. Baseline DeepRecSys, with further 8% improvement with LLC partitioning.

Different system configuration. We show a subset of our sensitivity study to different system configurations in Figure 17(b), illustrating the EMU improvement when the underlying system configuration is changed with different number of CPU cores, LLC ways, and memory bandwidth (GB/sec). As depicted, the benefits of Hera remains intact across diverse system platform configurations, achieving 30%/35%/18% EMU improvement for the shown configurations.

E. Design Overhead

Profiling/deployment cost. Hera is implemented as a profiling-based, feedback-driven scheduler, and the main design overhead comes from profiling the following two lookup tables: (a) QPS as a function of number of parallel workers (Figure 6) and (b) QPS as a function of LLC ways allocated (Figure 7). The profiling time taken to generate these two tables (T_{worker} and T_{LLC} , respectively) are:

$$T_{worker} = O(\text{number of CPU cores})$$

$$T_{LLC} = O(\text{number of LLC ways} \times \text{number of CPU cores})$$

Using our baseline system (Table II), T_{worker} and T_{LLC} takes less than 1 minute and 15 minutes per each model. As each data point can be collected completely independently, profiling and generating Figure 6 and Figure 7 across hundreds of models can easily be done within tens of minutes assuming thousands of compute nodes are available (which is readily accessible in cloud datacenters). Utilizing these two lookup tables as a 2D software array, generating the co-location affinity matrix in Figure 10(a) (Algorithm 1) even for hundreds of models takes less than one second using a single CPU core.

Deploying Hera across thousands of servers. Each inference server is deployed individually per-node and the execution of Hera’s cluster-wide scheduling algorithm (Algorithm 2) incurs less than 100 ms of latency, enabling scalable deployment in at-scale datacenters.

VIII. CONCLUSION

Hera is an application-aware co-location algorithm and resource management software for multi-tenant recommendation inference. We first conduct a characterization on multi-

tenant recommendations, uncovering its heterogeneous memory capacity and bandwidth demands. We then utilize such property to develop a profiling-based, feedback driven Hera runtime system that dynamically adapts resource allocation among multi-tenant workers for balancing latency throughput. Compared to state-of-the-art, Hera significantly improves effective machine utility while guaranteeing SLA.

REFERENCES

- [1] U. Gupta, C.-J. Wu, X. Wang, M. Naumov, B. Reagen, D. Brooks, B. Cottle, K. Hazelwood, M. Hempstead, B. Jia, H.-H. S. Lee, A. Malevich, D. Mudigere, M. Smelyanskiy, L. Xiong, and X. Zhang, “The Architectural Implications of Facebook’s DNN-based Personalized Recommendation,” in *Proceedings of the International Symposium on High-Performance Computer Architecture (HPCA)*, 2020.
- [2] T. Singhal, “Maximizing GPU Utilization For Datacenter Inference with NVIDIA TensorRT Inference Server.” NVIDIA Webinar, 2019.
- [3] M. Naumov, D. Mudigere, H.-J. M. Shi, J. Huang, N. Sundaraman, J. Park, X. Wang, U. Gupta, C.-J. Wu, A. G. Azzolini, D. Dzhulgakov, A. Malleevich, I. Cherniavskii, Y. Lu, R. Krishnamoorthi, A. Yu, V. Kondratenko, S. Pereira, X. Chen, W. Chen, V. Rao, B. Jia, L. Xiong, and M. Smelyanskiy, “Deep Learning Recommendation Model for Personalization and Recommendation Systems,” *arXiv preprint arXiv:1906.00091*, 2019.
- [4] H.-T. Cheng, L. Koc, J. Harmsen, T. Shaked, T. Chandra, H. Aradhye, G. Anderson, G. Corrado, W. Chai, M. Ispir, R. Anil, Z. Haque, L. Hong, V. Jain, X. Liu, and H. Shah, “Wide & Deep Learning for Recommender Systems,” in *Proceedings of the 1st workshop on deep learning for recommender systems*, 2016.
- [5] G. Zhou, X. Zhu, C. Song, Y. Fan, H. Zhu, X. Ma, Y. Yan, J. Jin, H. Li, and K. Gai, “Deep Interest Network for Click-Through Rate Prediction,” in *Proceedings of the ACM SIGKDD International Conference on Knowledge Discovery & Data Mining*, 2018.
- [6] G. Zhou, N. Mou, Y. Fan, Q. Pi, W. Bian, C. Zhou, X. Zhu, and K. Gai, “Deep Interest Evolution Network for Click-Through Rate Prediction,” in *Proceedings of the AAAI Conference on Artificial Intelligence*, 2019.
- [7] X. He, L. Liao, H. Zhang, L. Nie, X. Hu, and T.-S. Chua, “Neural Collaborative Filtering,” in *Proceedings of the international conference on world wide web*, 2017.
- [8] J. Park, M. Naumov, P. Basu, S. Deng, A. Kalaiah, D. Khudia, J. Law, P. Malani, A. Malevich, S. Nadathur, J. Pino, M. Schatz, A. Sidorov, V. Sivakumar, A. Tulloch, X. Wang, Y. Wu, H. Yuen, N. Diril, D. Dzhulgakov, K. Hazelwood, B. Jia, Y. Jia, L. Qiao, V. Rao, N. Rotem, S. Yoo, and M. Smelyanskiy, “Deep Learning Inference in Facebook Data Centers: Characterization, Performance Optimizations and Hardware Implications,” *arXiv preprint arXiv:1811.09886*, 2018.
- [9] Z. Deng, J. Park, P. T. P. Tang, H. Liu, J. Yang, H. Yuen, J. Huang, D. Khudia, X. Wei, E. Wen, D. Choudhary, R. Krishnamoorthi, C.-J. Wu, S. Nadathur, C. Kim, M. Naumov, S. Naghshineh, and M. Smelyanskiy, “Low-Precision Hardware Architectures Meet Recommendation Model Inference at Scale,” 2021.
- [10] D. Kalamkar, E. Georganas, S. Srinivasan, J. Chen, M. Shiryaev, and A. Heinecke, “Optimizing Deep Learning Recommender Systems’ Training On CPU Cluster Architectures,” *arXiv preprint arXiv:2005.04680*, 2020.
- [11] K. Hazelwood, S. Bird, D. Brooks, S. Chintala, U. Diril, D. Dzhulgakov, M. Fawzy, B. Jia, Y. Jia, A. Kalro, J. Law, K. Lee, J. Lu, P. Noordhuis, M. Smelyanskiy, L. Xiong, and X. Wang, “Applied Machine Learning at Facebook: A Datacenter Infrastructure Perspective,” in *Proceedings of the International Symposium on High-Performance Computer Architecture (HPCA)*, 2018.
- [12] R. Hwang, T. Kim, Y. Kwon, and M. Rhu, “Centaur: A Chiplet-Based, Hybrid Sparse-Dense Accelerator for Personalized Recommendations,” in *Proceedings of the International Symposium on Computer Architecture (ISCA)*, 2020.
- [13] U. Gupta, S. Hsia, V. Saraph, X. Wang, B. Reagen, G.-Y. Wei, H.-H. S. Lee, D. Brooks, and C.-J. Wu, “DeepRecSys: A System for Optimizing End-to-end At-scale Neural Recommendation Inference,” in *Proceedings of the International Symposium on Computer Architecture (ISCA)*, 2020.

- [14] U. Gupta, S. Hsia, J. Zhang, M. Wilkening, J. Pombra, H.-H. S. Lee, G.-Y. Wei, C.-J. Wu, and D. Brooks, "RecPipe: Co-Designing Models and Hardware to Jointly Optimize Recommendation Quality and Performance," in *Proceedings of the International Symposium on Microarchitecture (MICRO)*, 2021.
- [15] H. Liu, Q. Gao, J. Li, X. Liao, H. Xiong, G. Chen, W. Wang, G. Yang, Z. Zha, D. Dong, D. Dou, and H. Xiong, "JIZHI: A Fast and Cost-Effective Model-As-A-Service System for Web-Scale Online Inference at Baidu," in *Proceedings of the ACM SIGKDD International Conference on Knowledge Discovery & Data Mining*, 2021.
- [16] C. Olston, N. Fiedel, K. Gorovoy, J. Harmsen, L. Lao, F. Li, V. Rajashekhar, S. Ramesh, and J. Soyke, "TensorFlow-Serving: Flexible, High-Performance ML Serving," *arXiv preprint arXiv:1712.06139*, 2017.
- [17] NVIDIA, "NVIDIA Triton Inference Server." <https://developer.nvidia.com/nvidia-triton-inference-server>.
- [18] J. Mars, L. Tang, R. Hundt, K. Skadron, and M. L. Soffa, "BubbleUp: Increasing Utilization in Modern Warehouse Scale Computers via Sensible Co-Locations," in *Proceedings of the International Symposium on Microarchitecture (MICRO)*, 2011.
- [19] C. Delimitrou and C. Kozyrakis, "Paragon: QoS-Aware Scheduling for Heterogeneous Datacenters," in *Proceedings of the International Conference on Architectural Support for Programming Languages and Operating Systems (ASPLOS)*, 2013.
- [20] D. Lo, L. Cheng, R. Govindaraju, P. Ranganathan, and C. Kozyrakis, "Heracles: Improving Resource Efficiency at Scale," in *Proceedings of the International Symposium on Computer Architecture (ISCA)*, 2015.
- [21] H. Kasture and D. Sanchez, "UbiK: Efficient Cache Sharing with Strict QoS for Latency-Critical Workloads," in *Proceedings of the International Conference on Architectural Support for Programming Languages and Operating Systems (ASPLOS)*, 2014.
- [22] Y. Jiang, K. Tian, and X. Shen, "Combining Locality Analysis with Online Proactive Job Co-Scheduling in Chip Multiprocessors," in *International Conference on High-Performance Embedded Architectures and Compilers*, 2010.
- [23] Y. Jiang, K. Tian, X. Shen, J. Zhang, J. Chen, and R. Tripathi, "The Complexity of Optimal Job Co-Scheduling on Chip Multiprocessors and Heuristics-Based Solutions," *IEEE Transactions on Parallel and Distributed Systems*, 2010.
- [24] S. Chen, C. Delimitrou, and J. F. Martínez, "PARTIES: QoS-Aware Resource Partitioning for Multiple Interactive Services," in *Proceedings of the International Conference on Architectural Support for Programming Languages and Operating Systems (ASPLOS)*, 2019.
- [25] T. Patel and D. Tiwari, "CLITE: Efficient and QoS-Aware Co-location of Multiple Latency-Critical Jobs for Warehouse Scale Computers," in *Proceedings of the International Symposium on High-Performance Computer Architecture (HPCA)*, 2020.
- [26] R. Nishtala, V. Petrucci, P. Carpenter, and M. Sjalander, "Twig: Multi-Agent Task Management for Colocated Latency-Critical Cloud Services," in *Proceedings of the International Symposium on High-Performance Computer Architecture (HPCA)*, 2020.
- [27] Y. Choi and M. Rhu, "PREMA: A Predictive Multi-task Scheduling Algorithm For Preemptible Neural Processing Units," in *Proceedings of the International Symposium on High-Performance Computer Architecture (HPCA)*, 2020.
- [28] S. Ghodrati, B. H. Ahn, J. K. Kim, S. Kinzer, B. R. Yatham, N. Alla, H. Sharma, M. Alian, E. Ebrahimi, N. S. Kim, C. Young, and H. Esmaeilzadeh, "Planaria: Dynamic Architecture Fission for Spatial Multi-Tenant Acceleration of Deep Neural Networks," in *Proceedings of the International Symposium on Microarchitecture (MICRO)*, 2020.
- [29] Y. Kwon, Y. Lee, and M. Rhu, "TensorDIMM: A Practical Near-Memory Processing Architecture for Embeddings and Tensor Operations in Deep Learning," in *Proceedings of the International Symposium on Microarchitecture (MICRO)*, 2019.
- [30] L. Ke, U. Gupta, B. Y. Cho, D. Brooks, V. Chandra, U. Diril, A. Firoozshahian, K. Hazelwood, B. Jia, H.-H. S. Lee, M. Li, B. Maher, D. Mudigere, M. Naumov, M. Schatz, M. Smelyanskiy, X. Wang, B. Reagen, C.-J. Wu, M. Hempstead, and X. Zhang, "RecNMP: Accelerating Personalized Recommendation with Near-Memory Processing," in *Proceedings of the International Symposium on Computer Architecture (ISCA)*, 2020.
- [31] Y. Kwon, Y. Lee, and M. Rhu, "Tensor Casting: Co-Designing Algorithm-Architecture for Personalized Recommendation Training," in *Proceedings of the International Symposium on High-Performance Computer Architecture (HPCA)*, 2021.
- [32] B. Kim, J. Park, E. Lee, M. Rhu, and J. H. Ahn, "TRiM: Tensor Reduction in Memory," *IEEE Computer Architecture Letters*, 2020.
- [33] M. Wilkening, U. Gupta, S. Hsia, C. Trippel, C.-J. Wu, D. Brooks, and G.-Y. Wei, "RecSSD: Near Data Processing for Solid State Drive Based Recommendation Inference," in *Proceedings of the International Conference on Architectural Support for Programming Languages and Operating Systems (ASPLOS)*, 2021.
- [34] MLPerf, "MLPerf: A Broad ML Benchmark Suite for Measuring Performance of ML Software Frameworks, ML Hardware Accelerators, and ML Cloud Platforms." <https://github.com/mlperf/inference/tree/master/cloud>.
- [35] W. Zhao, J. Zhang, D. Xie, Y. Qian, R. Jia, and P. Li, "AIBox: CTR Prediction Model Training on A Single Node," in *Proceedings of the ACM International Conference on Information and Knowledge Management*, 2019.
- [36] X. Yi, Y.-F. Chen, S. Ramesh, V. Rajashekhar, L. Hong, N. Fiedel, N. Seshadri, L. Heldt, X. Wu, and H. Chi, "Factorized Deep Retrieval and Distributed TensorFlow Serving," in *Conference on Machine Learning and Systems*, 2018.
- [37] M. Lui, Y. Yetim, Ö. Özkan, Z. Zhao, S.-Y. Tsai, C.-J. Wu, and M. Hempstead, "Understanding Capacity-Driven Scale-Out Neural Recommendation Inference," *arXiv preprint arXiv:2011.02084*, 2020.
- [38] J. Hestness, N. Ardalani, and G. Diamos, "Beyond Human-Level Accuracy: Computational Challenges in Deep Learning," in *Proceedings of the Symposium on Principles and Practice of Parallel Programming (PPOPP)*, 2019.
- [39] SambaNova, "Surpassing State-of-the-Art Accuracy in Recommendation Models." <https://sambanova.ai/blog/surpassing-state-of-the-art-accuracy-in-recommendation-models/>, 2020.
- [40] W. Zhao, D. Xie, R. Jia, Y. Qian, R. Ding, M. Sun, and P. Li, "Distributed Hierarchical GPU Parameter Server for Massive Scale Deep Learning Ads Systems," in *Proceedings of Machine Learning and Systems*, 2020.
- [41] Intel, "Intel CMT CAT." <https://github.com/intel/intel-cmt-cat>.